Drosophila I-R hybrid dysgenesis is associated with catastrophic meiosis and abnormal zygote formation

Guillermo A. Orsi[1], Eric F. Joyce[2], Pierre Couble[1], Kim S. McKim[2] and Benjamin Loppin[1,*]

[1]Centre de Génétique Moléculaire et Cellulaire, CNRS UMR5534, University of Lyon, UCBL Lyon1, Villeurbanne, F-69100, France
[2]Waksman Institute and Department of Genetics, Rutgers University, 190, Frelinghuysen Rd, Piscataway NJ 08854, USA
*Author for correspondence (benjamin.loppin@univ-lyon1.fr)

Accepted 7 July 2010
Journal of Cell Science 123, 3515-3524

doi:10.1242/jcs.073890

Summary

The *Drosophila I-R* type of hybrid dysgenesis is a sterility syndrome (SF sterility) associated with the mobilization of the *I* retrotransposon in female germ cells. SF sterility results from a maternal-effect embryonic lethality whose origin has remained unclear since its discovery about 40 years ago. Here, we show that meiotic divisions in SF oocytes are catastrophic and systematically fail to produce a functional female pronucleus at fertilization. As a consequence, most embryos from SF females rapidly arrest their development with aneuploid or damaged nuclei, whereas others develop as non-viable, androgenetic haploid embryos. Finally, we show that, in contrast to mutants affecting the biogenesis of piRNAs, SF egg chambers do not accumulate persistent DNA double-strand breaks, suggesting that I-element activity might perturb the functional organization of meiotic chromosomes without triggering an early DNA damage response.

Key words: Hybrid dysgenesis, I element, Meiotic catastrophe, Haploid embryos, Meiotic DNA damage checkpoint

Introduction

Transposable elements (TEs) are essential structural and regulatory components of genomes. Their ability to transpose provides a fundamental source of genetic variation but also represents a potential threat for genome integrity. Genomes have deployed a diversity of epigenetic defensive mechanisms against TEs and their concerted action results in the global, efficient and heritable repression of mobile elements throughout generations (Aravin et al., 2007; Siomi et al., 2008; Slotkin et al., 2007). In *Drosophila*, epigenetic control of TEs depends on histone modifications, chromatin structure, small RNA-based transcriptional silencing and DNA methylation (Aravin et al., 2007; Josse et al., 2007; Klenov et al., 2007; Dramard et al., 2007; Phalke et al., 2009; Klattenhoff et al., 2007; Klattenhoff et al., 2009; Li et al., 2009; Malone et al., 2009). Recent literature has abundantly described the mechanisms of Piwi-interacting small RNAs (piRNAs) biogenesis, as well as their essential role for the repression of TEs in germ cells (Brennecke et al., 2007; Vagin et al., 2006; Saito et al., 2006; Aravin et al., 2007; Siomi et al., 2008; Klattenhoff and Theurkauf, 2008). Accordingly, several families of TEs are derepressed in the germline of mutants affecting the piRNA pathway (Vagin et al., 2006; Chambeyron et al., 2008; Pane et al., 2007; Lim and Kai, 2007; Chen et al., 2007; Klattenhoff et al., 2007; Klattenhoff et al., 2009; Vagin et al., 2004). Remarkably, all these mutants are viable but induce female sterility associated with a complex phenotype including defects in germline stem cell maintenance, accumulation of germline DNA damage and aberrant egg axial patterning (Klattenhoff and Theurkauf, 2008). However, it is difficult to determine the actual contribution of TE activity to their complex sterility phenotype (Klattenhoff et al., 2007; Thomson and Lin, 2009).

In *Drosophila*, massive and deleterious TE germline mobilization is also observed in the progeny of certain intraspecific crosses. This phenomenon, known as hybrid dysgenesis, has long been recognized as a powerful experimental model for the study of TE regulation in a wild-type background (Bregliano et al., 1980). *Drosophila* hybrid dysgenesis systems are usually characterized by a severe gonadal atrophy in both sexes, resulting in sterility. These include the *D. melanogaster P-M* (P element) and *H-E* (hobo element) systems, as well as a hybrid dysgenesis in *D. virilis*, which involves several families of TEs (Kidwell and Novy, 1979; Blackman et al., 1987; Yannopoulos et al., 1987; Petrov et al., 1995; Blumenstiel and Hartl, 2005). The *I-R* type of hybrid dysgenesis is unique as it only occurs in females and does not result from a defective ovarian development. Instead, dysgenic females lay a normal amount of eggs but the resulting embryos fail to hatch (Picard and L'Héritier, 1971). The causative factor of this non-Mendelian female sterility is the *I* element, a 5.4 kb, non-LTR retrotransposon of the LINE (long interspersed nucleotidic element) superfamily of transposable elements (Bucheton et al., 1984). Most *D. melanogaster* strains are so-called *Inducer* (*I*) strains and contain about 10 transposition-competent but transcriptionally silenced *I* elements. Such functional *I* elements are absent from *Reactive* (*R*) strains that were established before the recent worldwide invasion of this retrotransposon in natural populations (Bucheton et al., 2002). Maternal transmission of piRNAs has been proposed to underlie the epigenetic repression of TEs revealed by *Drosophila* hybrid dysgenesis systems (Blumenstiel and Hartl, 2005; Brennecke et al., 2008; Chambeyron et al., 2008). In the case of the *I-R* system, maternal epigenetic protection is largely reduced in *R* strains, resulting in the expression of paternally transmitted *I* elements in the naive germline of dysgenic females (Brennecke et al., 2008; Chambeyron et al., 2008).

I-R hybrid dysgenesis occurs when *I* males are crossed with *R* females. The female progeny of this dysgenic cross, called SF (stérilité femelle) females, usually display a strong sterility phenotype associated with derepression of *I* elements. In addition, the *I-R* syndrome is characterized by a high mutation rate as well

as chromosomal non-disjunctions and rearrangements (Bucheton et al., 2002). In contrast to SF females, the genetically identical RSF females obtained from the reverse cross (*R* males with *I* females) show much lower expression of *I* elements and are fully fertile (Picard and L'Héritier, 1971; Bucheton et al., 2002). From the early work of Picard et al. (Picard et al., 1977) and Lavige (Lavige, 1986), it was established that embryos produced by SF females died through a strict maternal effect and frequently presented abnormal syncytial divisions. However, despite extensive research on this system, the nature of SF sterility has remained enigmatic since its discovery (Picard and L'Héritier, 1971).

In this paper, we have undertaken a detailed cytological study of *I-R* hybrid dysgenesis to determine the origin of SF sterility. Our study revealed that meiotic divisions are catastrophic in SF oocytes and eggs. This highly penetrant phenotype prevents the integration of the full set of maternal chromosomes in the zygote, resulting in non-viable embryos. We also show that, in contrast to mutants affecting the biogenesis of piRNAs, SF germ cells do not accumulate massive DNA damage during early oogenesis, suggesting that *I* activity perturbs the functional organization of meiotic chromosomes without activating the early germline DNA damage response.

Results

Meiotic catastrophe in eggs of SF females

We performed a cytological study of SF eggs and embryos to understand the nature of SF maternal-effect embryonic lethality. We used SF females that were not older than a week as SF sterility decreases progressively with age (see below). Consistent with early cytological studies (Lavige, 1986), we observed that a majority of syncytial SF embryos contained catastrophic mitotic figures with isolated or broken chromosomes and asynchronously dividing nuclei of various sizes (Fig. 1). In addition, in SF embryos, we observed that the polar body did not form the typical triploid rosette and contained many fragmented chromosomes (Fig. 1D–F). This last aspect of the phenotype suggested that meiosis was defective in SF eggs. We then turned to late oocytes to observe the first meiotic division. In *Drosophila*, the mature stage-14 oocyte is arrested in metaphase of meiosis I (King, 1970). To visualize the organization of meiotic chromosomes and the first meiotic spindle, we used control and SF females expressing the fluorescent centromeric protein EGFP-Cid (Schuh et al., 2007) or the microtubule-associated Jupiter-GFP (Buszczak et al., 2007), respectively. In fixed control stage-14 oocytes (n=30), meiotic chromosomes appeared as a slightly elongated mass of chromatin with non-exchange chromosomes occasionally separated towards the spindle poles (Fig. 2) (Theurkauf and Hawley, 1992). In about 80% of SF oocytes (22/28), the chromatin appeared fragmented and/or abnormally distributed into several small masses (Fig. 2). Some of these masses of chromatin were associated with an EGFP-Cid spot, whereas others were not, thus suggesting the presence of fragmented chromosomes. These isolated or fragmented chromosomes formed miniature spindle-like structures as revealed with the Jupiter-GFP marker (Fig. 2). In the rest of the SF oocytes (6/28), the first meiotic division was apparently normal, although the low resolution of meiosis I chromosomes did not allow the detection of possible more subtle defects.

We then analyzed very early SF eggs to observe the second meiotic division and pronuclear formation. Strikingly, meiosis II in SF eggs was almost systematically abnormal with bridges of chromatin connecting the separating chromatids in anaphase and telophase (Fig. 3C,D; Table 1). This defective separation of chromatids was followed by chromosome fragmentation and unequal segregation of meiotic products. Notably, the loss of genetic material in the female pronucleus was obvious at the pronuclear apposition stage. In control RSF eggs, apposed pronuclei appeared identical in size (Fig. 3E). In SF eggs, however, the female pronucleus was either small, fragmented in several smaller nuclei or, in some instances, did not form at all (Fig. 3F,G; data not shown). We thus concluded that, in eggs from SF females, defective meiotic divisions compromised the formation of a normal female pronucleus.

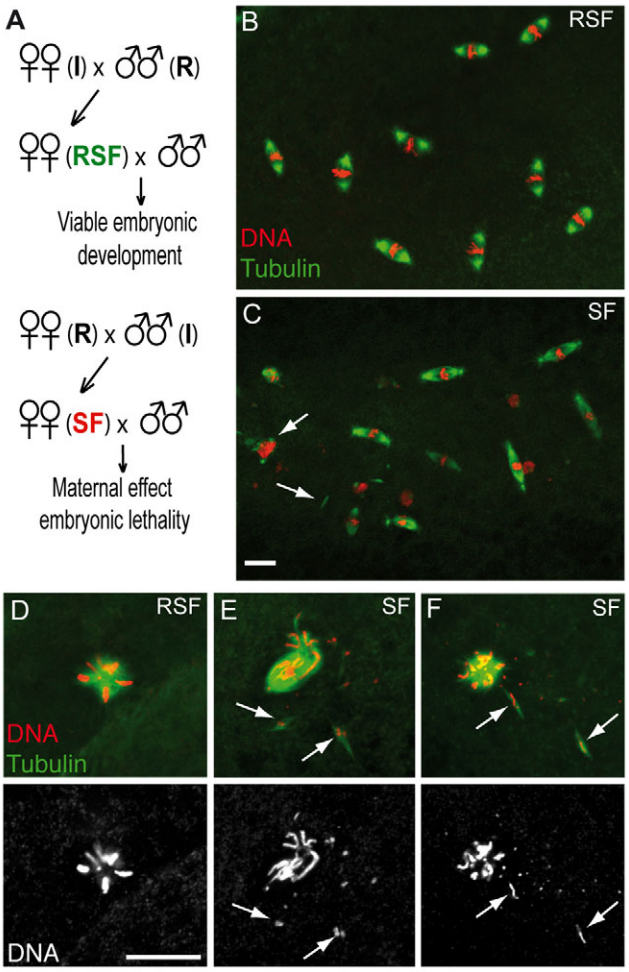

Fig. 1. The maternal-effect embryonic lethality associated with *I-R* hybrid dysgenesis. (**A**) Crossing scheme to obtain RSF (upper) and SF (lower) females. SF females lay eggs but the resulting embryos die before hatching. Genetically identical RSF females are fully fertile. (**B**,**C**) Confocal images of early syncytial embryos from RSF (B) or SF (C) females stained for Tubulin (green) and DNA (red). In contrast to the normal nuclear divisions observed in RSF embryos, SF embryos contain asynchronously dividing nuclei of various sizes and fragmented chromosomes (arrows). (**D–F**) In RSF embryos (D), fused polar bodies form a typical rosette of condensed chromosomes. In SF embryos (E,F), polar body organization is abnormal and many chromosomes are lost or fragmented (arrows). Scale bars: 15 μm.

Embryos from SF females develop with paternal chromosomes

In *Drosophila* fertilized eggs, pronuclei do not fuse but instead remain apposed during the first zygotic S phase and the paternal

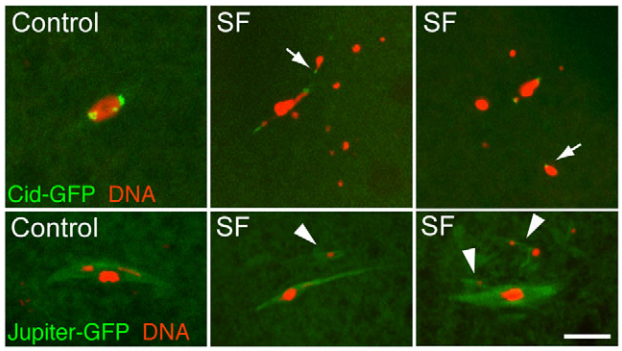

Fig. 2. Meiosis I is catastrophic in oocytes from SF females. Confocal images of meiosis I in stage-14 oocytes from females expressing the indicated marker. Control females are from the transgenic *EGFP-Cid* line and *Jupiter-GFP* line. SF females were obtained by crossing inducer *EGFP-Cid* or *Jupiter-GFP* males with *Charolles* females at 25°C. At day 5 of adult life, ovaries were dissected, fixed and stained for DNA (red). Scale bar: 10 µm. (**Top**) EGFP-tagged centromeric histone Cid (EGFP-Cid) marks centromeres in meiosis I chromosomes. In control oocytes, chromosomes show aligned centromeres in prometaphase. In SF oocytes, chromosomes appear fragmented or mislocalized. Centromeres are indicated with arrows. (**Bottom**) The control is an anastral first meiotic spindle in prometaphase marked with microtubule-associated Jupiter-GFP. In SF oocytes, mini-spindles organize around mislocalized or fragmented chromosomes (arrowheads).

and maternal sets of chromosomes enter mitosis as separate entities within a common mitotic spindle (Sonnenblick, 1950). In a majority of SF embryos at first mitosis, we observed that the spindle did not contain the full complement of chromosomes compared with RSF zygotes (Fig. 3H,I; Table 1). In other cases, some chromosomes were excluded from the spindle or lagged behind in anaphase of the first division (Fig. 3J,K; Table 1). To determine the identity of these absent or abnormal chromosomes, we stained SF eggs with an antibody directed against acetylated forms of histone H4 that preferentially marks paternal chromatin (Loppin et al., 2005a). We observed that, in SF eggs, from the pronuclear apposition until the end of the first zygotic division, the damaged or late chromosomes were systematically less-intensely stained than the unaffected chromosomes (Fig. 4A-F). In some cases, a single haploid set of strongly stained chromosomes was present at the first mitosis (Fig. 4E). We confirmed these observations by analyzing the progeny of transgenic SF females expressing the recombinant histone variant H3.3-Flag, a specific marker of paternal chromosomes at fertilization (Bonnefoy et al., 2007; Orsi et al., 2009). This experiment clearly confirmed the specific defective integration of maternal chromosomes in SF zygotes (supplementary material Fig. S1).

As previously reported by Picard et al. (Picard et al., 1977) and Lavige (Lavige, 1986), we observed that approximately 7% (n=1134) of SF embryos died at a late developmental stage as revealed by the fact that they turned brown after death and showed signs of organogenesis and cuticle deposition. By contrast, the rest of the unhatched eggs remained whitish, suggesting that they arrested development before cellularization (Fig. 4K). In the *Drosophila* mutant *maternal haploid* (*mh*), paternal chromosomes are unable to divide in anaphase of the first mitosis and form a chromatin bridge (Santamaria and Gans, 1980; Loppin et al., 2001). This frequently results in catastrophic early mitoses and most embryos die after a few rounds of nuclear divisions. However, a fraction of embryos escape this early arrest and

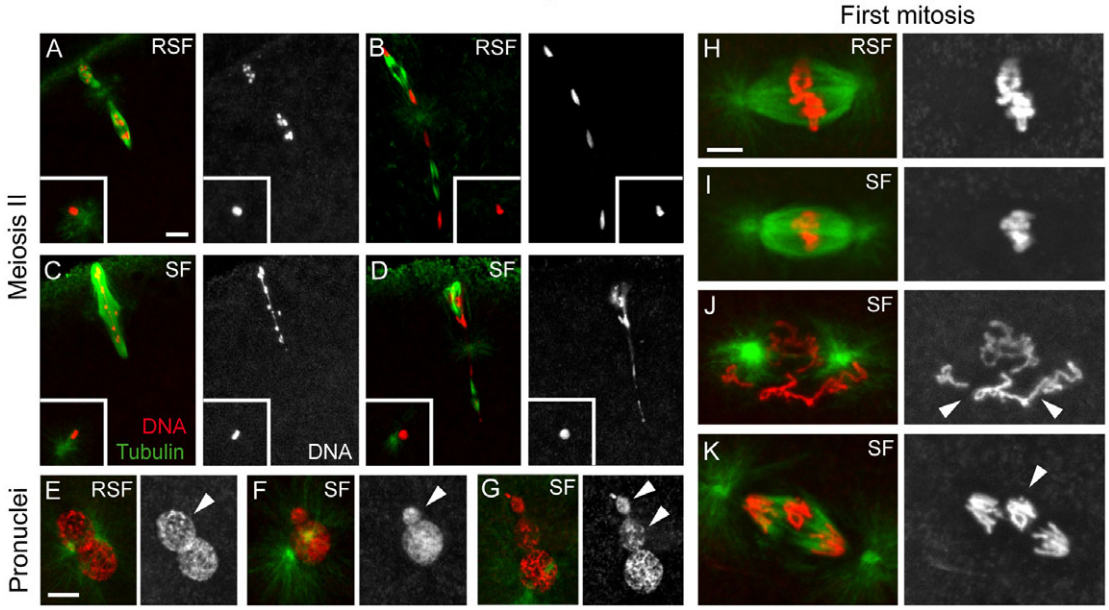

Fig. 3. Catastrophic meiosis and abnormal zygote formation in eggs from SF females. Confocal images of eggs and early embryos stained for Tubulin (green) and DNA (red). (**A–D**) Meiosis figures are shown with dorsal egg periphery at the top and the anterior end to the left. The corresponding male pronuclei are shown in insets. (A,B) RSF eggs in anaphase (A) or telophase (B) of the second meiotic division. (C,D) Meiosis II in SF eggs is catastrophic. Note the chromatin bridges in anaphase (C) and the unequal chromosome segregation in telophase (D). Loss of genetic material in the two innermost meiotic products is obvious in D. (**E**) Pronuclear apposition in an RSF egg. (**F**,**G**) In SF eggs, the female pronucleus looks abnormally small (F) or fragmented into several smaller nuclei (G). The female pronuclei are indicated with arrowheads. (**H–K**) First zygotic division. Metaphase of the first zygotic division in an RSF egg (H) containing the paternal and maternal chromosomes. First mitosis in an SF egg with either a reduced number of chromosomes (I), with chromosomes that appear excluded from the spindle (arrowheads in J) or with lagging chromosomes in anaphase (arrowheads in K). Scale bars: 10 µm.

Table 1. Phenotype quantification of SF eggs and embryos

	Meiosis II		First zygotic division		Cycle 2 –7 embryos		
	n	Abnormal (%)	*n*	Abnormal (%)	*n*	Aneuploid (%)	Haploid (%)
SF	40	97.5	56	96.4	90	82.2	11.1
RSF	41	2.4	25	0	50	0	0

SF or RSF females grown at 25°C were allowed to lay eggs between days 4 and 6 after emergence (day 1). Eggs at 0–1 hours were collected, fixed and stained for DNA. Phenotypes of SF eggs (meiosis II and zygote) and early embryos are described in the Results. *n*, the total number of eggs and/or embryos analyzed.

develop as non-viable, haploid gynogenetic embryos (Loppin et al., 2001). At the cytological level, early development of SF embryos appeared similar to *mh* embryos, with catastrophic syncytial divisions forming chromatin bridges (Fig. 1C; supplementary material Fig. S2). In addition, a minority of SF embryos developed beyond the blastoderm stage and contained normal mitotic figures but the nuclei were about half the size of control diploid nuclei (Fig. 4G-J). To demonstrate that these escaper embryos were actually haploid androgenetic embryos, we crossed SF females with males homozygous for the *K81* paternal effect mutation, which prevents the formation of functional paternal chromosomes in the progeny (Fuyama, 1984; Yasuda et al., 1995; Loppin et al., 2005b). As expected, these SF females failed to produce any brown embryos during their first week, confirming that late embryos from SF females developed with paternal chromosomes (Fig. 4L,M; supplementary material Table S1). In conclusion, our results demonstrated that most embryos from SF females die early with catastrophic mitoses, whereas a minority escape this early arrest as haploid androgenetic embryos.

Defective karyosome formation in SF oocytes

The meiotic phenotype observed in SF females prompted us to analyze the structure of the oocyte nucleus during SF oogenesis. In *Drosophila*, female meiosis initiates in region 2A of the germarium, at the anterior tip of each ovariole. After meiotic recombination, in later egg chambers, the oocyte nucleus enlarges while the condensed maternal chromosomes in prophase I of meiosis remain packaged within a subnuclear structure known as the karyosome (Spradling, 1993). In stage 6–9 control oocytes stained for DNA, the karyosome appeared as a round condensed structure within the unstained oocyte nucleus (Fig. 5A). By striking contrast, we observed that the karyosome was disorganized in a majority of SF oocytes (Fig. 5A; supplementary material Fig. S2). Typically, the SF karyosomes were fragmented and stretched along the inner side of the oocyte nuclear envelope. A remarkable and well-described feature of SF sterility is its modulation by age and temperature. Indeed, SF sterility is highest in young females but their fertility is progressively restored as they age (see supplementary material Table S1) (Picard and L'Héritier, 1971). In addition, SF sterility is strongest and lasts longer at relatively cooler temperatures and fertility can be transiently restored after a heat treatment (Bucheton, 1979). Interestingly, we observed that the penetrance and severity of the karyosome phenotype decreased with the age of SF females. In addition, most karyosomes were severely affected when SF females where placed at 18°C for 36 hours before dissection, whereas a heat treatment at 30°C dramatically suppressed the phenotype (Fig. 5B,C). Taken together, these observations suggest that defective karyosome formation in SF oocytes results in abnormal meiotic divisions.

SF germ cells do not accumulate unrepaired DNA double-strand breaks

In *Drosophila* female germ cells, the accumulation of unrepaired DNA double-strand breaks (DSBs) can trigger the activation of a well-characterized ATR-Chk2 (Mei-41-Lok) DNA damage response (Ghabrial and Schupbach, 1999; Abdu et al., 2002). In mutants that affect the repair of meiotic DNA DSBs, activation of the Chk2 checkpoint leads to a complex cellular response. This includes a specific disorganization of the karyosome and a strong egg ventralization phenotype that results from defective accumulation of the signaling protein Gurken in the oocyte (Ghabrial and Schupbach, 1999; Abdu et al., 2002). Interestingly, the Chk2 checkpoint is activated in the female germline of piRNA pathway mutants (Chen et al., 2007; Klattenhoff et al., 2007). In addition, these mutants are associated with egg patterning defects and defective karyosome formation (supplementary material Fig. S3) (Chen et al., 2007; Klattenhoff et al., 2007). Genetic analyses have demonstrated that, in these mutants, the checkpoint is not activated by meiotic DSBs, thus opening the possibility that these DNA damages could be induced by the activity of derepressed TEs (Chen et al., 2007; Klattenhoff et al., 2007; Klattenhoff et al., 2009).

As mutant stocks are generally not available in a reactive background, the activation of the checkpoint in SF germ cells could not be genetically tested. We thus examined the dorsal patterning of SF eggs to check for indications of DNA damage response. We observed that a fraction of SF eggs displayed a weak ventralization phenotype. In fact, fusion of egg dorsal appendages was only observed with very young SF females not older than 3 days (Table 2; Fig. 4K, arrow). Importantly, after a few days, SF females that were still fully sterile produced almost 100% of eggs with wild-type appendages. By clear contrast, *aub* or *armi* mutant females produced a majority of severely ventralized eggs throughout their life (Table 2). Interestingly, Van De Bor et al. (Van De Bor et al., 2005) have shown that *I* and *gurken* (*grk*) transcripts compete for the same RNA localization machinery in SF egg chambers, resulting in defective dorsoventral axis specification. This mechanism could indeed account for the ventralization of eggs produced by young SF females, where strong *I* transcription is expected to efficiently perturb *grk* mRNA localization. In conclusion, the egg patterning analysis did not support the hypothesis of early Chk2 checkpoint activation in SF germ cells. However, we wished to directly evaluate the impact of *I*-element activity on DNA integrity during early oogenesis. We thus stained SF and control ovaries with antibodies against the phosphorylated form of histone H2Av (γ-His2Av), which associates with DNA DSBs (Mehrotra and McKim, 2006). In wild-type or RSF ovaries, γ-His2Av foci were observed in oocytes of germarium regions 2A and 2B but were no longer detected in late-pachytene oocytes in their region 3 egg chambers (Fig. 6). In region 3 oocytes from *aub* mutant females, late-pachytene nuclei accumulated numerous γ-His2Av foci, as previously reported (Klattenhoff et al., 2007). By clear contrast,

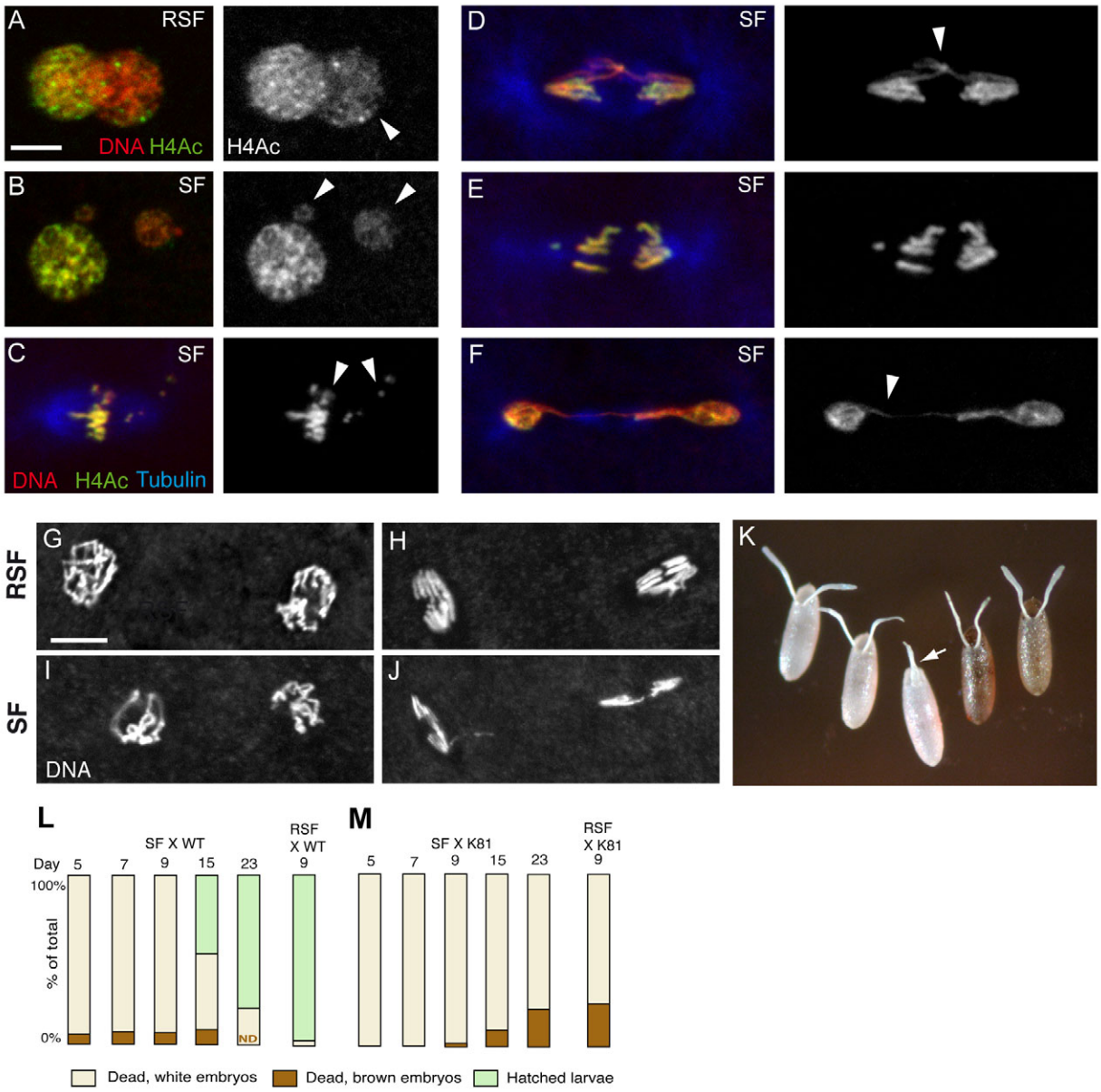

Fig. 4. Early loss of maternal chromosomes in SF embryos. (**A–J**) Confocal images of eggs and embryos stained with the indicated markers. (A,B) RSF (A) and SF (B) pronuclei stained with an anti-acetylated H4 antibody (green or white) that preferentially marks paternal chromatin (Loppin et al., 2005a). The female pronuclei are indicated with arrowheads. (C–F) First mitosis in SF eggs stained for acetylated H4 (green or white), DNA (red) and Tubulin (blue). Maternal chromosomes appear red and paternal chromosomes are yellow. Maternal chromosomes are abnormally positioned in the spindle or fragmented (arrowheads in C), lagging behind in anaphase or telophase (arrowheads in D and F) or absent (E). (G–J) Diploid nuclei from blastoderm RSF embryos in prophase (G) and anaphase (H). SF embryos that reach the blastoderm stage contain haploid nuclei (I, prophase; J, anaphase). Nuclei were stained with Propidium Iodide. (**K**) Unhatched eggs from SF females appear either whitish, indicative of early developmental arrest (the three eggs on the left), or brown, indicative of haploid development (the two eggs on the right). The arrow points to a weakly ventralized egg with the dorsal appendages fused at their base. (**L**) Diagrams showing the color phenotype of unhatched embryos produced from the same batch of SF females at the indicated days (day 1 is the day of emergence). Note that SF females progressively recover fertility as they age. ND, not determined. (**M**) When SF females are crossed with *K81* mutant males, brown embryos are not produced during the first week of life. Note that RSF females as well as aging SF females crossed with *K81* males produce an expected fraction of haploid gynogenetic embryos that turn brown after death. Scale bars: 10 µm. Numbers of examined embryos are in supplementary material Table S1.

such an accumulation of DNA DSBs was not observed in SF region 3 oocytes (n=10). In fact, half of region 3 SF oocytes were devoid of γ-His2Av foci, as in RSF controls. Interestingly, however, a few (1–3) γ-His2Av foci were observed in the other half of the late-pachytene SF oocytes but they never persisted beyond that stage. Thus, *I* activity either occasionally delays the repair of meiotic DSBs or, alternatively, generates a small number of non-persistent DSBs unrelated to meiotic recombination.

BicD aggregates are not observed in SF egg chambers

In wild-type inducer ovaries, endogenously expressed *I* transcripts are essentially sequestered in nurse cell nuclear foci in a piRNA-

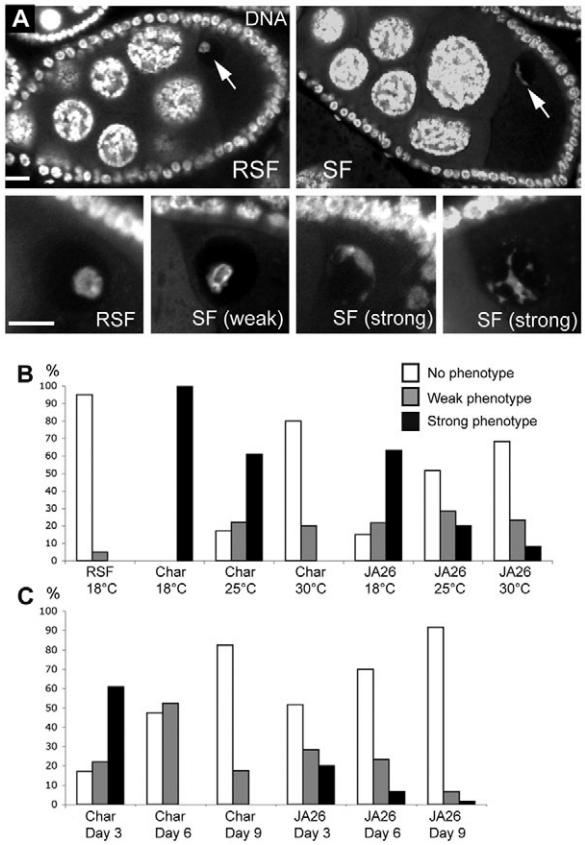

Fig. 5. Defective karyosome formation in SF oocytes. (**A**) Confocal images of stage 7–8 egg chambers dissected from RSF or SF females and stained for DNA (top). Egg chamber stages are from King (King, 1970). The oocyte is on the right, the karyosome is indicated with an arrow. (Bottom) In oocytes from RSF females, the karyosome appears spheric and condensed within the unstained oocyte nucleus. In SF oocytes, the karyosome is frequently abnormal, being slightly heterogeneous or elongated in aspect (weak phenotype) or displaying a severe distortion, fragmentation or attachment to the nuclear envelope (strong phenotype). (**B**) Effect of temperature on SF karyosome phenotype. Two-day-old RSF or SF females obtained at 25°C using the *Charolles* or *JA26* reactive stocks were placed at the indicated temperature for 36 hours before ovary dissection and DNA staining. For each condition, a minimum of 40 karyosomes from stage 6–9 oocytes were observed and classified according to the phenotypic classes described in A. Results are shown as a percentage of all observed karyosomes. (**C**) Effect of age on SF karyosome phenotype. SF females obtained at 25°C using the *Charolles* or *JA26* reactive stocks were dissected at the indicated age and ovaries were stained for DNA. Karyosome phenotype was analyzed as in B. Note that the same 25°C, 3-day-old SF female data is shown in B and C. Scale bars: 20 µm.

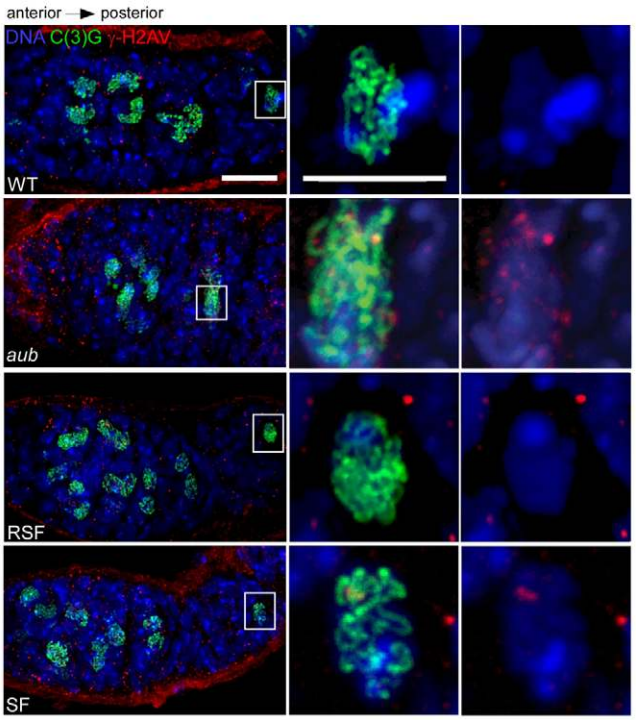

Fig. 6. γ-His2AvD distribution in the SF germline. Confocal images of wild-type (WT), aub^{QC42} or aub^{HN} (*aub*), RSF and SF germaria stained to visualize DNA (blue), C(3)G (green) and γ-His2AvD (red). Full views of germaria with their anterior tip on the left are shown in the left panels. Increased magnifications of late-pachytene oocytes (insets) are on the right. In WT and RSF germaria, γ-H2AvD foci are not detected in late-pachytene oocytes [identified by the C(3)G staining], indicating that meiotic DNA double-strand breaks are repaired at this stage. In generally disorganized *aub* mutant germaria, where oocyte determination is delayed, >10 γ-His2AvD foci accumulate in late-pachytene oocyte nuclei, shown here in an early region 3 oocyte. In SF germaria, 0–3 γ-His2AvD foci are observed in late-pachytene oocytes. A total of 10 late-pachytene oocytes were examined for each genotype. Scale bars: 5 µm.

dependent manner (Chambeyron et al., 2008), whereas overexpressed GFP-labeled *I* transcripts have been shown to accumulate in cytoplasmic particles called pi-bodies that localize around nurse cell nuclei (Lim et al., 2009). In SF egg chambers, *I* transcripts are essentially transported in the oocyte (Seleme et al., 2005; Chambeyron et al., 2008). Recently, it has been shown that large ribonucleoprotein (RNP) aggregates of the dynein-motor machinery form in egg chambers of piRNA biogenesis mutants (Navarro et al., 2009). Interestingly, injected *I* transcripts accumulate in these aggregates, suggesting that they could serve as degradation sites for retrotransposon products, in the absence of piRNA biogenesis (Navarro et al., 2009). Furthermore, these authors have also shown that formation of these dynein aggregates was largely dependent upon the activation of the Chk2 checkpoint.

To investigate the possibility that these structures could form in SF egg chambers, we stained ovaries with anti-BicD or anti-Orb antibodies that were shown to accumulate in dynein aggregates (Navarro et al., 2009). We indeed observed aggregates in a large majority of *aub* or *armi* mutant egg chambers. By clear contrast, however, Orb or BicD aggregates were only rarely observed in SF and RSF egg chambers (Fig. 7A,B; data not shown). We conclude that *I*-element activity is not sufficient to trigger the formation of these aggregates in dysgenic ovaries. In the course of these experiments, we observed that the oocyte marker BicD was abnormally distributed in the germinal vesicle of a majority of *aub* and *armi* mutant stage 6–9 egg chambers (Fig. 7A,C). This phenotype was fully rescued in *aub mnk* double-mutant females, indicating that it was dependent on checkpoint activation (Fig. 7A,C). Importantly, we observed that, in SF and RSF oocytes, BicD was normally excluded from the germinal vesicle. Taken together, these results reinforce the conclusion that SF sterility is independent of Chk2 checkpoint activation and downstream cellular responses.

Table 2. Egg patterning of SF eggs

Maternal genotype	Dorsal appendage phenotype (%)			Hatch rate (%)	*n*
	Wild-type	Fused	Absent		
aub^{HN}/aub^{QC42}	23.1	52.4	24.5	0	481
aub^{HN} mnk^{P6}/aub^{QC42} mnk^{P6}	99.2	0.8	0	0	354
$armi^{1}/armi^{72.1}$	0.2	11.7	88.1	0	463
mnk^{P6}/mnk^{P6}; $armi^{1}/armi^{72.1}$	76.6	16.1	7.3	0	137
RSF	100.0	0	0	96.2	498
SF (days 1–3)	69.3	30.4	0.3	0	743
SF (days 4–5)	99.2	0.8	0	0.2	651

Egg ventralization phenotypes are described in Staeva-Vieira et al. (Staeva-Vieira et al., 2003). SF females that emerged on day 1 were crossed with wild-type males and eggs from the same females were collected and analyzed after day 3 (days 1–3) and day 5 (days 4–5). The phenotype of eggs from other females remained unchanged over the same period of 5 days (data not shown).

Discussion

Extensive research on *Drosophila* hybrid dysgenesis systems has brought an essential contribution to the paradigm of TE epigenetic silencing. However, these models have comparatively received limited attention regarding the actual effect of TE activity in germ cells. In this context, the maternal-effect embryonic lethality associated with SF sterility appeared particularly difficult to link with *I* activity during oogenesis. In this study, we have shown that embryo lethality is a consequence of catastrophic meiosis in SF eggs. The loss or fragmentation of meiotic chromosomes leads to abnormal female pronucleus formation and prevents the subsequent development of viable diploid embryos. Instead, embryos from SF females initiate development with missing or damaged maternal chromosomes or with only the set of intact paternal chromosomes.

In contrast to the dramatic phenotype observed in eggs and embryos, SF oogenesis appeared relatively undisturbed by *I*-element activity. Our observation of meiosis prophase I progression in SF germaria has revealed the presence of a small number of non-persistent γ-His2Av foci in late-pachytene oocytes. These foci, supposedly associated with unrepaired DSBs, are thus the earliest phenotypic manifestation of *I* activity in SF germ cells that we were able to detect. Meiotic DSBs are normally repaired before the end of prophase and γ-His2Av foci are only exceptionally observed in wild-type region 3 oocytes (Mehrotra and McKim, 2006). The foci observed in SF oocytes could possibly result from a delay in the repair of DSBs induced by meiotic recombination, implying that *I* activity might disturb or slow down the normal repair process of meiotic DSBs. Alternatively, these DSBs could be directly generated by *I* retrotransposition. Indeed, in mammalian cells, retrotransposition of the *I*-related LINE 1 (L1) elements generates DNA DSBs associated with γ-His2AX foci (Bourc'his and Bestor, 2004; Belgnaoui et al., 2006; Gasior et al., 2006; Soper et al., 2008).

Whatever the origin of this DNA damage in early SF germ cells, they do not appear sufficient to trigger the activation of the Chk2-dependent checkpoint, at least as it is described for mutants affecting the repair of meiotic DSBs (Ghabrial and Schupbach, 1999; Abdu et al., 2002). For comparison, in certain hypomorphic alleles of meiotic DSB repair genes, the meiotic checkpoint is not activated despite the presence of about 7–10 persistent γ-His2Av foci (E.F.J. and K.S.M., unpublished data). The egg patterning analysis of SF eggs also supported the apparent absence of meiotic checkpoint activation in SF germ cells. Indeed, the weak ventralization phenotype observed with very young females disappeared after a few days despite the fact that dysgenic females remained fully sterile.

By contrast, SF egg chambers displayed a clear karyosome phenotype that was highly correlated with sterility. The morphology defect of SF karyosomes was reminiscent of the karyosomes in piRNA mutants. In these mutants, activation of the Chk2 checkpoint

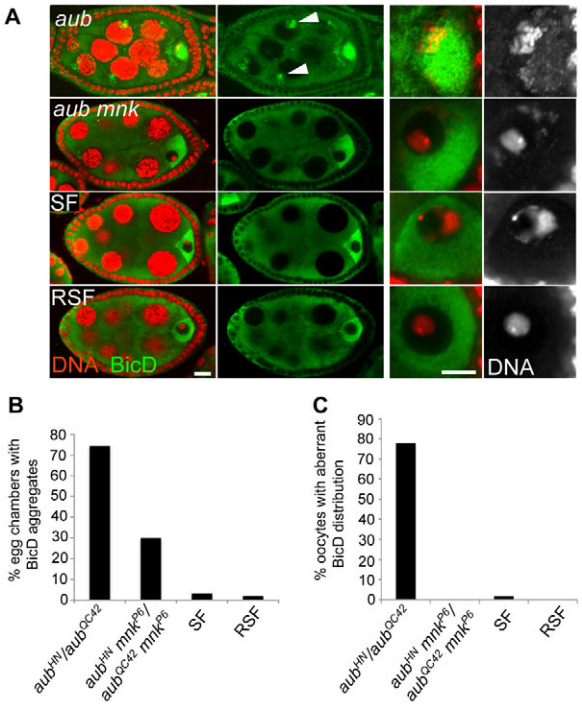

Fig. 7. BicD distribution is not affected in SF ovaries. (**A**) Confocal images of stage-9 egg chambers from aub^{HN}/aub^{QC42} (*aub*), aub^{HN} mnk^{P6}/aub^{QC42} mnk^{P6} (*aub mnk*), SF and RSF females raised at 25°C. At days 3–5 of adult life, ovaries were dissected, fixed and stained for BicD (green) and DNA (red). BicD aggregates accumulate in egg chambers from control *aub* mutants (arrowheads) but not from double *aub mnk* mutants, SF or RSF females (left panels). Magnification of germinal vesicles of the same stage and genotype are shown in the right panels. Note that BicD is abnormally distributed within the germinal vesicle in *aub* mutant oocytes, whereas it is normally excluded from the oocyte nucleus in *aub mnk*, SF and RSF egg chambers. (**B**) Quantification of BicD aggregates. For each type of ovary, a minimum of 70 egg chambers at stages 6–9 were evaluated for presence or absence of BicD aggregates. (**C**) Quantification of aberrant BicD distribution. For each type of ovary, a minimum of 60 oocytes at stages 6–9 were analyzed. Note that karyosomes show a strong phenotype in *aub* mutants but appear normally shaped in *aub mnk* oocytes. Scale bars: 10 µm.

is at least partially responsible for this phenotype, in a way similar to mutants affecting the repair of meiotic breaks (Ghabrial and Schupbach, 1999; Abdu et al., 2002; Staeva-Vieira et al., 2003). Indeed, we have observed that 97% (n=62) and 26% (n=94) of *aub mnk* and *mnk armi* karyosomes had a morphology rescued to wild-type, respectively (Fig. 7; data not shown).

Interestingly, DNA damage accumulation and karyosome defects in the absence of strong dorsoventral patterning defects have been described for mutants that affect both meiotic DNA damage repair and checkpoint signaling, such as *hus1* and *brca2* (Abdu et al., 2007; Klovstad et al., 2008). Similarly, germline derepression of TEs in the *tejas* mutant does not affect egg polarity (Patil and Kai, 2010). We thus cannot exclude that the karyosome defect in SF oocytes could reflect a partial or late DNA damage response, which would not trigger other known hallmarks of checkpoint activation, including egg ventralization. Indeed, in SF ovaries, *I* transcripts and ORF1 protein are first detected in germarium region 2A but they reach their highest levels in later-stage oocytes, where they presumably accumulate as RNPs (Seleme et al., 1999; Seleme et al., 2005). At these stages, however, any accumulation of DNA DSBs might go undetected with γ-His2Av antibodies. In this model, the DNA damage response could still cause the observed karyosome defect but would occur too late to significantly disturb Grk protein oocyte accumulation and dorsoventral axis specification.

In the alternative possibility, accumulation of *I* RNPs in the oocyte could directly affect karyosome formation without inducing any DNA damage response. However, and surprisingly, *I* products accumulate in the perinuclear cytoplasm of SF oocytes and do not appear to enter the nuclear compartment at cytologically detectable levels (Seleme et al., 1999; Seleme et al., 2005). Accordingly, GFP-tagged ORF1p remains cytoplasmic when transiently expressed in *Drosophila* cultured cells (Rashkova et al., 2002). Thus, only a minor fraction of *I* RNPs is expected to enter the oocyte nucleus in order to complete the retrotransposition process. This situation contrasts with the clear nuclear accumulation of L1 RNPs in *mael*$^{-/-}$ mutant mouse spermatocytes associated with DNA damage and chromosome asynapsis (Soper et al., 2008). In SF ovaries, we did not detect any gross defect in the distribution of the SC protein C(3)G in oocytes (supplementary material Fig. S4). However, the low resolution obtained with this kind of analysis (compared with mouse spermatocytes, for instance) cannot rule out the presence of undetected chromosome synapsis defects.

The modest effect of *I* activity on DNA integrity during early SF oogenesis contrasted with the situation observed in piRNA mutants where many TEs, including *I*, are derepressed. However, the origin of DNA damage in piRNA pathway mutants is not clear and the involvment of TEs in generating these breaks remains to be established (Chen et al., 2007; Klattenhoff et al., 2007; Klattenhoff and Theurkauf, 2008; Thomson and Lin, 2009). Genetic inactivation of the checkpoint does not restore the fertility of piRNA pathway mutant females (Table 2) (Klattenhoff et al., 2007). It thus indicates that additional, checkpoint-independent defects cause the female sterility in these mutants. Interestingly, embryos from *aub mnk* females display a specific and severe disorganization of cleavage nuclei that could explain the observed maternal-effect lethality (Blumenstiel et al., 2008). Furthermore, in *aub* and *spn-E* mutants, the *HeT-A* and *TART* retroelements involved in telomere maintenance are upregulated in the female germline and their retrotransposition to broken chromosome termini is increased, with potential consequences on chromosome stability (Savitsky et al., 2006). Finally, Piwi-family proteins are also involved in the biogenesis or processing of piRNAs directed against the 3′ UTR of a broad set of cellular transcripts, with possible regulatory functions (Robine et al., 2009). The overall phenotype of piRNA pathway mutants is thus expected to reflect this functional complexity, in contrast to *I-R* hybrid dysgenesis, where a single type of element is activated.

The meiotic defects we observed in SF oocytes and eggs are probably related to the chromosome rearrangements and non-disjunctions associated with *I-R* hybrid dysgenesis. Rearrangements are probably generated after illegitimate homologous recombination events between integrating *I* elements (Busseau et al., 1989; Prudhommeau and Proust, 1990; Proust et al., 1992). Considering the fact that these chromosomal aberrations were obtained in viable progeny from SF females, we suppose that more detrimental and frequent rearrangements are produced when SF females are still fully sterile. The accumulation of chromosomal rearrangements in oocyte nuclei could probably affect meiotic divisions by notably inducing non-disjunction and chromosome fragmentation events. In this model, the progressive *I* repression established in aging SF females would reduce the probability of these events occurring until oocyte chromosome architecture becomes compatible with normal meiosis.

Materials and Methods

Drosophila stocks

The w^{1118} standard inducer stock and the strong reactive wild-type stock *Charolles* were used to set up control or dysgenic crosses, unless otherwise specified. The *JA26 y w* reactive stock was provided by Alain Pelisson (Institute de Génétique Humaine, Montpellier, France). The *EGFP-Cid* stock (Schuh et al., 2007) and the *Jupiter-GFP* insertion (Buszczak et al., 2007) were obtained from Stefan Heidmann (University of Bayreuth, Bayreuth, Germany) and from the Carnegie Protein Trap Stock Collection (http://flytrap.med.yale.edu/), respectively. The mnk^{P6} stock was a gift from Tin Tin Su (Brodsky et al., 2004). The following alleles were obtained from the Bloomington *Drosophila* Stock Center at Indiana University (http://flystocks.bio.indiana.edu/): $armi^{1}$ and $armi^{72.1}$ (Cook et al., 2004), aub^{HN} and aub^{QC42} (Schupbach and Wieschaus, 1991), $krimp^{f06583}$ (Lim and Kai, 2007) and $mael^{r20}$ (Clegg et al., 1997). The following heterozygous or hemizygous females were used in this study: $armi^{1}$ $armi^{72.1}$ (*armi*), aub^{HN} aub^{QC42} (*aub*), $krimp^{f06583}$ *Df(2R)Exel6063* (*krimp*) and $mael^{r20}$ *Df(3L)ED230* (*mael*). The $K81^{2}$ paternal-effect embryonic lethal mutant is a small, viable deficiency that completely removes the *ms(3)K81* gene (Yasuda et al., 1995). *aub mnk* or *mnk armi* double-mutant females were obtained by standard crossing techniques and meiotic recombination.

Crosses and egg phenotype analysis

Control and dysgenic crosses were set up at the appropriate temperature using equal numbers of freshly emerged virgin males and females that were kept together throughout the experiment. Eggs were collected on agar plates, counted and, if necessary, the dorsal appendage phenotype was examined by direct observation under a stereomicroscope. Embryos were then allowed to develop for 3 days at 25°C before hatching rate and brown/white phenotype determination.

Egg collection, ovary dissection and immunofluorescence

Females that were no older than 1 week were allowed to lay eggs on agar plates in the presence of males at 25°C. Eggs were dechorionated in bleach and fixed as described (Loppin et al., 2001). Ovaries were dissected in TBST (TBS-0.15%, Triton X-100), fixed in a 1:1 mixture of heptane: 4% paraformaldehyde in PBS, rinsed in TBST and were immediately incubated with the primary antibodies as previously described (Bonnefoy et al., 2007). Antibodies and dilutions used were: anti-α-Tubulin (Sigma, T9026, 1/500); anti-H4Ac (Chemicon International, AB3062, 1/200); anti-Flag (Sigma, F3165, 1/1000); anti-H3K14Ac (Millipore, 06-911, 1/500); anti-C(3)G (kindly provided by R. S. Hawley, 1/500) (Page and Hawley, 2001); anti-γ-His2AvD (1/500) (Mehrotra and McKim, 2006); and anti-BicD (Developmental Studies Hybridoma Bank, 1B11-s, 1/200). DNA was stained with Propidium Iodide or Hoechst. Confocal images were acquired using either a LSM510 microscope (Carl Zeiss) or a Leica SP2 (for Fig. 5) and were processed with Adobe Photoshop software.

Karyosome defect assay

To analyze the effect of temperature on karyosome phenotype, 1-day-old SF females were kept at 25°C for 2 days and were then placed at 18°C, 25°C or 30°C for 36 hours before ovary dissection. To analyze the effect of age, SF females that were obtained at 25°C were aged for 3, 6 or 9 days before dissection. Stage 6–9 oocytes

stained with Propidium Iodide and H3K14Ac were observed under a confocal microscope and karyosomes were classified into three phenotypical categories as described in Fig. 4. For each condition, a minimum of 40 karyosomes was observed.

We are grateful to Alain Pelisson, Scott Hawley, Stefan Heidmann, Tin Tin Su, the Carnegie Protein Trap Stock Collection and the Bloomington Stock Center for flies and antibodies. We would like to thank Béatrice Horard, Stéphane Ronsseray, Anne Laurençon, Marion Delattre and Silke Jensen for discussions and critical reading of the manuscript, and Emmanuel Gauthier for providing some of the cited literature. We also thank Jérôme Schmitt for technical assistance. Confocal microscopy was performed with the help of the Centre Technologique des Microstructures. Work in the laboratory of B.L. was supported by the CNRS and by a grant from the ANR (ANR-08-BLAN-0139-01). Work in the laboratory of K.S.M. was supported by a grant from the NSF. G.A.O. is supported by a doctoral fellowship from the French Ministry of Education and Research.

Supplementary material available online at
http://jcs.biologists.org/cgi/content/full/123/20/3515/DC1

References

Abdu, U., Brodsky, M. and Schupbach, T. (2002). Activation of a meiotic checkpoint during *Drosophila* oogenesis regulates the translation of Gurken through Chk2/Mnk. *Curr. Biol.* **12**, 1645-1651.

Abdu, U., Klovstad, M., Butin-Israeli, V., Bakhrat, A. and Schupbach, T. (2007). An essential role for *Drosophila* hus1 in somatic and meiotic DNA damage responses. *J. Cell Sci.* **120**, 1042-1049.

Aravin, A. A., Hannon, G. J. and Brennecke, J. (2007). The Piwi-piRNA pathway provides an adaptive defense in the transposon arms race. *Science* **318**, 761-764.

Belgnaoui, S. M., Gosden, R. G., Semmes, O. J. and Haoudi, A. (2006). Human LINE-1 retrotransposon induces DNA damage and apoptosis in cancer cells. *Cancer Cell Int.* **6**, 13.

Blackman, R. K., Grimaila, R., Koehler, M. M. and Gelbart, W. M. (1987). Mobilization of hobo elements residing within the decapentaplegic gene complex: suggestion of a new hybrid dysgenesis system in *Drosophila melanogaster*. *Cell* **49**, 497-505.

Blumenstiel, J. P. and Hartl, D. L. (2005). Evidence for maternally transmitted small interfering RNA in the repression of transposition in *Drosophila virilis*. *Proc. Natl. Acad. Sci. USA* **102**, 15965-15970.

Blumenstiel, J. P., Fu, R., Theurkauf, W. E. and Hawley, R. S. (2008). Components of the RNAi machinery that mediate long-distance chromosomal associations are dispensable for meiotic and early somatic homolog pairing in *Drosophila melanogaster*. *Genetics* **180**, 1355-1365.

Bonnefoy, E., Orsi, G. A., Couble, P. and Loppin, B. (2007). The essential role of *Drosophila* HIRA for de novo assembly of paternal chromatin at fertilization. *PLoS Genet.* **3**, 1991-2006.

Bourc'his, D. and Bestor, T. H. (2004). Meiotic catastrophe and retrotransposon reactivation in male germ cells lacking Dnmt3L. *Nature* **431**, 96-99.

Bregliano, J. C., Picard, G., Bucheton, A., Pelisson, A., Lavige, J. M. and L'Heritier, P. (1980). Hybrid dysgenesis in *Drosophila melanogaster*. *Science* **207**, 606-611.

Brennecke, J., Aravin, A. A., Stark, A., Dus, M., Kellis, M., Sachidanandam, R. and Hannon, G. J. (2007). Discrete small RNA-generating loci as master regulators of transposon activity in *Drosophila*. *Cell* **128**, 1089-1103.

Brennecke, J., Malone, C. D., Aravin, A. A., Sachidanandam, R., Stark, A. and Hannon, G. J. (2008). An epigenetic role for maternally inherited piRNAs in transposon silencing. *Science* **322**, 1387-1392.

Brodsky, M. H., Weinert, B. T., Tsang, G., Rong, Y. S., McGinnis, N. M., Golic, K. G., Rio, D. C. and Rubin, G. M. (2004). *Drosophila melanogaster* MNK/Chk2 and p53 regulate multiple DNA repair and apoptotic pathways following DNA damage. *Mol. Cell. Biol.* **24**, 1219-1231.

Bucheton, A. (1979). Non-Mendelian female sterility in *Drosophila melanogaster*: influence of aging and thermic treatments. III. Cumulative effects induced by these factors. *Genetics* **93**, 131-142.

Bucheton, A., Paro, R., Sang, H. M., Pelisson, A. and Finnegan, D. J. (1984). The molecular basis of I-R hybrid dysgenesis in *Drosophila melanogaster*: identification, cloning, and properties of the I factor. *Cell* **38**, 153-163.

Bucheton, A., Busseau, I. and Teninges, D. (2002). I Elements in *Drosophila melanogaster*. In *Mobile DNA II* (ed. N. L. Craig) pp. 796-812. Washington, DC: ASM Press.

Busseau, I., Pelisson, A. and Bucheton, A. (1989). I elements of *Drosophila melanogaster* generate specific chromosomal rearrangements during transposition. *Mol. Gen. Genet.* **218**, 222-228.

Buszczak, M., Paterno, S., Lighthouse, D., Bachman, J., Planck, J., Owen, S., Skora, A. D., Nystul, T. G., Ohlstein, B., Allen, A. et al. (2007). The carnegie protein trap library: a versatile tool for *Drosophila* developmental studies. *Genetics* **175**, 1505-1531.

Chambeyron, S., Popkova, A., Payen-Groschene, G., Brun, C., Laouini, D., Pelisson, A. and Bucheton, A. (2008). piRNA-mediated nuclear accumulation of retrotransposon transcripts in the *Drosophila* female germline. *Proc. Natl. Acad. Sci. USA* **105**, 14964-14969.

Chen, Y., Pane, A. and Schupbach, T. (2007). Cutoff and aubergine mutations result in retrotransposon upregulation and checkpoint activation in *Drosophila*. *Curr. Biol.* **17**, 637-642.

Clegg, N. J., Frost, D. M., Larkin, M. K., Subrahmanyan, L., Bryant, Z. and Ruohola-Baker, H. (1997). maelstrom is required for an early step in the establishment of *Drosophila* oocyte polarity: posterior localization of grk mRNA. *Development* **124**, 4661-4671.

Cook, H. A., Koppetsch, B. S., Wu, J. and Theurkauf, W. E. (2004). The Drosophila SDE3 homolog armitage is required for oskar mRNA silencing and embryonic axis specification. *Cell* **116**, 817-829.

Dramard, X., Heidmann, T. and Jensen, S. (2007). Natural epigenetic protection against the I-factor, a *Drosophila* LINE retrotransposon, by remnants of ancestral invasions. *PLoS ONE* **2**, e304.

Fuyama, Y. (1984). Gynogenesis in *Drosophila melanogaster*. *Jpn J. Genet.* **59**, 91-96.

Gasior, S. L., Wakeman, T. P., Xu, B. and Deininger, P. L. (2006). The human LINE-1 retrotransposon creates DNA double-strand breaks. *J. Mol. Biol.* **357**, 1383-1393.

Ghabrial, A. and Schupbach, T. (1999). Activation of a meiotic checkpoint regulates translation of Gurken during *Drosophila* oogenesis. *Nat. Cell Biol.* **1**, 354-357.

Ivanovska I., Khandan T., Ito T. and Orr-Weaver T. L. (2005) A histone code in meiosis: the histone kinase, NHK-1, is required for proper chromosomal architecture in *Drosophila* oocytes. Genes Dev. **19**, 2571-2582.

Josse, T., Teysset, L., Todeschini, A. L., Sidor, C. M., Anxolabehere, D. and Ronsseray, S. (2007). Telomeric trans-silencing: an epigenetic repression combining RNA silencing and heterochromatin formation. *PLoS Genet.* **3**, 1633-1643.

Kidwell, M. G. and Novy, J. B. (1979). Hybrid dysgenesis in *Drosophila melanogaster*: sterility resulting from gonadal dysgenesis in the P-M system. *Genetics* **92**, 1127-1140.

King, R. C. (1970). *Ovarian Development in Drosophila Melanogaster.* New York: Academic Press.

Klattenhoff, C. and Theurkauf, W. (2008). Biogenesis and germline functions of piRNAs. *Development* **135**, 3-9.

Klattenhoff, C., Bratu, D. P., McGinnis-Schultz, N., Koppetsch, B. S., Cook, H. A. and Theurkauf, W. E. (2007). *Drosophila* rasiRNA pathway mutations disrupt embryonic axis specification through activation of an ATR/Chk2 DNA damage response. *Dev. Cell* **12**, 45-55.

Klattenhoff, C., Xi, H., Li, C., Lee, S., Xu, J., Khurana, J. S., Zhang, F., Schultz, N., Koppetsch, B. S., Nowosielska, A. et al. (2009). The *Drosophila* HP1 homolog Rhino is required for transposon silencing and piRNA production by dual-strand clusters. *Cell* **138**, 1137-1149.

Klenov, M. S., Lavrov, S. A., Stolyarenko, A. D., Ryazansky, S. S., Aravin, A. A., Tuschl, T. and Gvozdev, V. A. (2007). Repeat-associated siRNAs cause chromatin silencing of retrotransposons in the *Drosophila melanogaster* germline. *Nucleic Acids Res.* **35**, 5430-5438.

Klovstad, M., Abdu, U. and Schupbach, T. (2008). *Drosophila* brca2 is required for mitotic and meiotic DNA repair and efficient activation of the meiotic recombination checkpoint. *PLoS Genet.* **4**, e31.

Lavige, J. M. (1986). I-R system of hybrid dysgenesis in *Drosophila melanogaster*: further data on the arrest of development of the embryos from SF females. *Biol. Cell* **56**, 207-216.

Li, C., Vagin, V. V., Lee, S., Xu, J., Ma, S., Xi, H., Seitz, H., Horwich, M. D., Syrzycka, M., Honda, B. M. et al. (2009). Collapse of germline piRNAs in the absence of Argonaute3 reveals somatic piRNAs in flies. *Cell* **137**, 509-521.

Lim, A. K. and Kai, T. (2007). Unique germ-line organelle, nuage, functions to repress selfish genetic elements in *Drosophila melanogaster*. *Proc. Natl. Acad. Sci. USA* **104**, 6714-6719.

Loppin, B., Berger, F. and Couble, P. (2001). Paternal chromosome incorporation into the zygote nucleus is controlled by maternal haploid in *Drosophila*. *Dev. Biol.* **231**, 383-396.

Loppin, B., Bonnefoy, E., Anselme, C., Laurencon, A., Karr, T. L. and Couble, P. (2005a). The histone H3.3 chaperone HIRA is essential for chromatin assembly in the male pronucleus. *Nature* **437**, 1386-1390.

Loppin, B., Lepetit, D., Dorus, S., Couble, P. and Karr, T. L. (2005b). Origin and neofunctionalization of a *Drosophila* paternal effect gene essential for zygote viability. *Curr. Biol.* **15**, 87-93.

Malone, C. D., Brennecke, J., Dus, M., Stark, A., McCombie, W. R., Sachidanandam, R. and Hannon, G. J. (2009). Specialized piRNA pathways act in germline and somatic tissues of the *Drosophila* ovary. *Cell* **137**, 522-535.

Mehrotra, S. and McKim, K. S. (2006). Temporal analysis of meiotic DNA double-strand break formation and repair in *Drosophila* females. *PLoS Genet.* **2**, e200.

Navarro, C., Bullock, S. and Lehmann, R. (2009). Altered dynein-dependent transport in piRNA pathway mutants. *Proc. Natl. Acad. Sci. USA* **106**, 9691-9696.

Orsi, G. A., Couble, P. and Loppin, B. (2009). Epigenetic and replacement roles of histone variant H3.3 in reproduction and development. *Int. J. Dev. Biol.* **53**, 231-243.

Page, S. L. and Hawley, R. S. (2001). c(3)G encodes a *Drosophila* synaptonemal complex protein. *Genes Dev.* **15**, 3130-3143.

Pane, A., Wehr, K. and Schupbach, T. (2007). zucchini and squash encode two putative nucleases required for rasiRNA production in the *Drosophila* germline. *Dev. Cell* **12**, 851-862.

Patil, V. S. and Kai, T. (2010). Repression of retroelements in *Drosophila* germline via piRNA pathway by the Tudor domain protein Tejas. *Curr. Biol.* **20**, 1-7.

Petrov, D. A., Schutzman, J. L., Hartl, D. L. and Lozovskaya, E. R. (1995). Diverse transposable elements are mobilized in hybrid dysgenesis in *Drosophila virilis*. *Proc. Natl. Acad. Sci. USA* **92**, 8050-8054.

Phalke, S., Nickel, O., Walluscheck, D., Hortig, F., Onorati, M. C. and Reuter, G. (2009). Retrotransposon silencing and telomere integrity in somatic cells of *Drosophila* depends on the cytosine-5 methyltransferase DNMT2. *Nat. Genet.* **41**, 696-702.

Picard, G. and L'Héritier, P. (1971). A maternally inherited factor inducing sterility in *Drosophila melanogaster*. *Drosophila inf. Serv.* **46**, 54.

Picard, G., Lavige, J. M., Bucheton, A. and Bregliano, J. C. (1977). Non mendelian female sterility in *Drosophila melanogaster*: physiological pattern of embryo lethality. *Biol. Cell.* **29**, 89-98.

Proust, J., Prudhommeau, C., Ladeveze, V., Gotteland, M. and Fontyne-Branchard, M. C. (1992). I-R hybrid dysgenesis in *Drosophila melanogaster*. Use of in situ hybridization to show the association of I factor DNA with induced sex-linked recessive lethals. *Mutat. Res.* **268**, 265-285.

Prudhommeau, C. and Proust, J. (1990). I-R hybrid dysgenesis in *Drosophila melanogaster*: nature and site specificity of induced recessive lethals. *Mutat. Res.* **230**, 135-157.

Rashkova, S., Karam, S. E. and Pardue, M. L. (2002). Element-specific localization of *Drosophila* retrotransposon Gag proteins occurs in both nucleus and cytoplasm. *Proc. Natl. Acad. Sci. USA* **99**, 3621-3626.

Robine, N., Lau, N. C., Balla, S., Jin, Z., Okamura, K., Kuramochi-Miyagawa, S., Blower, M. D. and Lai, E. C. (2009). A broadly conserved pathway generates 3′UTR-directed primary piRNAs. *Curr. Biol.* **19**, 2066-2076.

Saito, K., Nishida, K. M., Mori, T., Kawamura, Y., Miyoshi, K., Nagami, T., Siomi, H. and Siomi, M. C. (2006). Specific association of Piwi with rasiRNAs derived from retrotransposon and heterochromatic regions in the *Drosophila* genome. *Genes Dev.* **20**, 2214-2222.

Santamaria, P. and Gans, M. (1980). Chimaeras of *Drosophila melanogaster* obtained by injection of haploid nuclei. *Nature* **287**, 143-144.

Savitsky, M., Kwon, D., Georgiev, P., Kalmykova, A. and Gvozdev, V. (2006). Telomere elongation is under the control of the RNAi-based mechanism in the *Drosophila* germline. *Genes Dev.* **20**, 345-354.

Schuh, M., Lehner, C. F. and Heidmann, S. (2007). Incorporation of *Drosophila* CID/CENP-A and CENP-C into centromeres during early embryonic anaphase. *Curr. Biol.* **17**, 237-243.

Schupbach, T. and Wieschaus, E. (1991). Female sterile mutations on the second chromosome of *Drosophila melanogaster*. II. Mutations blocking oogenesis or altering egg morphology. *Genetics* **129**, 1119-1136.

Seleme, M. C., Busseau, I., Malinsky, S., Bucheton, A. and Teninges, D. (1999). High-frequency retrotransposition of a marked I factor in *Drosophila melanogaster* correlates with a dynamic expression pattern of the ORF1 protein in the cytoplasm of oocytes. *Genetics* **151**, 761-771.

Seleme, M. C., Disson, O., Robin, S., Brun, C., Teninges, D. and Bucheton, A. (2005). In vivo RNA localization of I factor, a non-LTR retrotransposon, requires a cis-acting signal in ORF2 and ORF1 protein. *Nucleic Acids Res.* **33**, 776-785.

Siomi, M. C., Saito, K. and Siomi, H. (2008). How selfish retrotransposons are silenced in *Drosophila* germline and somatic cells. *FEBS Lett.* **582**, 2473-2478.

Slotkin, R. K. and Martienssen, R. (2007). Transposable elements and the epigenetic regulation of the genome. *Nat. Rev. Genet.* **8**, 272-285.

Sonnenblick, B. P. (1950). The early embryology of *Drosophila melanogaster*. In *Biology of Drosophila* (ed. M. Demerc), pp. 62-167. New York: John Wiley and Sons.

Soper, S. F., van der Heijden, G. W., Hardiman, T. C., Goodheart, M., Martin, S. L., de Boer, P. and Bortvin, A. (2008). Mouse maelstrom, a component of nuage, is essential for spermatogenesis and transposon repression in meiosis. *Dev. Cell* **15**, 285-297.

Spradling, A. C. (1993). Developmental genetics of oogenesis. In *The Development of Drosophila melanogaster* (ed. M. Bate and A. Martinez-Arias), pp. 1-70. Cold Spring Harbor, NY: Cold Spring Harbor Laboratory Press.

Staeva-Vieira, E., Yoo, S. and Lehmann, R. (2003). An essential role of DmRad51/SpnA in DNA repair and meiotic checkpoint control. *EMBO J.* **22**, 5863-5874.

Theurkauf, W. E. and Hawley, R. S. (1992). Meiotic spindle assembly in *Drosophila* females: behavior of nonexchange chromosomes and the effects of mutations in the nod kinesin-like protein. *J. Cell Biol.* **116**, 1167-1180.

Thomson, T. and Lin, H. (2009). The biogenesis and function of PIWI proteins and piRNAs: progress and prospect. *Annu. Rev. Cell Dev. Biol.* **25**, 355-376.

Vagin, V. V., Klenov, M. S., Kalmykova, A. I., Stolyarenko, A. D., Kotelnikov, R. N. and Gvozdev, V. A. (2004). The RNA interference proteins and vasa locus are involved in the silencing of retrotransposons in the female germline of *Drosophila melanogaster*. *RNA Biol.* **1**, 54-58.

Vagin, V. V., Sigova, A., Li, C., Seitz, H., Gvozdev, V. and Zamore, P. D. (2006). A distinct small RNA pathway silences selfish genetic elements in the germline. *Science* **313**, 320-324.

Van De Bor, V., Hartswood, E., Jones, C., Finnegan, D. and Davis, I. (2005). gurken and the I factor retrotransposon RNAs share common localization signals and machinery. *Dev. Cell* **9**, 51-62.

Yannopoulos, G., Stamatis, N., Monastirioti, M., Hatzopoulos, P. and Louis, C. (1987). hobo is responsible for the induction of hybrid dysgenesis by strains of Drosophila melanogaster bearing the male recombination factor 23.5MRF. *Cell* **49**, 487-495.

Yasuda, G. K., Schubiger, G. and Wakimoto, B. T. (1995). Genetic characterization of ms (3) K81, a paternal effect gene of *Drosophila melanogaster*. *Genetics* **140**, 219-229.